

Micromagic clock: microwave clock based on atoms in an engineered optical lattice

K. Bely and A. Derevianko

Department of Physics, University of Nevada, Reno, Nevada 89557

V. A. Dzuba and V. V. Flambaum

School of Physics, University of New South Wales, Sydney, 2052, Australia

(Dated: October 26, 2018)

We propose a new class of atomic microwave clocks based on the hyperfine transitions in the ground state of aluminum or gallium atoms trapped in optical lattices. For these elements *magic* wavelengths exist at which both levels of the hyperfine doublet are shifted at the same rate by the lattice laser field, cancelling its effect on the clock transition. Our analysis of various systematic effects shows that, while offering an improved control over systematic errors, the accuracy of the proposed microwave clock is competitive to that of the state-of-the-art primary frequency standard.

PACS numbers: 06.30.Ft, 37.10.Jk, 31.15.A-

The present definition of the unit of time, the second, is based on the frequency of the microwave transition between two hyperfine levels of Cs atom. The Cs atomic clocks date back more than a half of a century. The accuracy of the standard has been substantially improved over the years culminating in a fountain clock apparatus operated around the world [1, 2]. Recently, it has been realized that the accuracy and stability of atomic clocks can be substantially improved by trapping atoms in a standing wave of a laser light (optical lattices) operated at a certain “magic” wavelength [3, 4]. The laser wavelength is tuned so that the differential light perturbations of the two clock levels vanishes exactly. In other words, while remaining confined (this eliminates the Doppler and recoil shifts), the atoms behave spectroscopically as if they were in a vacuum. Millions of atoms can be trapped and interrogated simultaneously, vastly improving stability of the clock. Such setup was experimentally realized [5, 6, 7] for optical frequency clock transitions in divalent atoms yielding accuracies competitive to the fountain clocks [7]. However, because these lattice clocks operate at an optical frequency, to relate to the definition of the second, they require state of the art frequency combs to bridge the optical frequency to the microwave counters.

Here we extend the fruitful ideas of the optical lattice clocks to microwave frequencies. We propose a new class of atomic microwave clocks based on the hyperfine transitions in the ground state of aluminum or gallium atoms trapped in optical lattices. We determine the magic wavelengths and analyze various systematic effects. We find that the accuracy of the proposed clockwork is at least competitive to that of the most-precise clocks. Moreover, compared to a large chamber of the fountain clock, the atoms are confined to a tiny volume offering improved control over systematic errors. A relative compactness of the clockwork could benefit space-craft applications such as navigation systems and precision tests of fundamental theories.

The microwave clockwork involves two atomic levels of the same hyperfine manifold. The transition frequency is monitored and ultimately translated into a time mea-

surement. We envision the following experimental setup: the atoms are trapped in a 1D optical lattice formed by counter-propagating laser beams of linear polarization and frequency ω_L . The quantizing magnetic field \mathbf{B} is directed either along the direction of the laser propagation \hat{k} or along the polarization vector $\hat{\varepsilon}$. The clock states are commonly labeled as $|n(IJ)FM_F\rangle$, where I is the nuclear spin, J is the electronic angular momentum, and F is the total angular momentum, $\mathbf{F} = \mathbf{J} + \mathbf{I}$, with M_F being its projection on the quantization axis and n encompassing the remaining quantum numbers. To minimize a sensitivity to stray magnetic fields and residual circular polarization of the laser light, we choose to work with the $M_F = 0$ components.

Under the influence of the laser each clock level is perturbed. The relevant energy shifts are parameterized in terms of the dynamic scalar, $\alpha_a^S(\omega_L)$, and tensor, $\alpha_a^T(\omega_L)$, polarizabilities. The corresponding expression reads

$$\delta E_{n(IJ)FM_F}^{\text{Stark}}(\omega_L) = -\left(\frac{1}{2}\mathcal{E}_0\right)^2 \left[\alpha_{n(IJ)F}^S(\omega_L) + \xi(\theta) \alpha_{n(IJ)F}^T(\omega_L) \frac{3M_F^2 - F(F+1)}{F(2F-1)} \right], \quad (1)$$

where $\xi(\theta) = (3\cos^2\theta - 1)/2$, θ being the angle between \mathbf{B} and $\hat{\varepsilon}$. In particular, $\xi = 1$ for $\mathbf{B} \parallel \hat{\varepsilon}$ and $\xi = -1/2$ for $\mathbf{B} \parallel \hat{k}$ geometries. \mathcal{E}_0 is the amplitude of the laser field. While arriving at these expressions we required that the Zeeman splittings in the B-field are much larger than the off-diagonal matrix of the optical Hamiltonian, a condition which can be easily attained experimentally.

The clock frequency is modified by the difference

$$\delta\nu^{\text{Stark}}(\omega_L) = \frac{1}{h} \left(\delta E_{n(IJ)F'M'_F}^{\text{Stark}}(\omega_L) - \delta E_{n(IJ)F''M''_F}^{\text{Stark}}(\omega_L) \right)$$

We require that at a certain, “magic”, laser frequency ω_L^* , this laser-induced differential shift vanishes: $\delta\nu(\omega_L^*) = 0$.

The “magic” cancellation mechanism depends on the frequency dependence of underlying polarizabilities. We

use perturbation theory and expand the polarizabilities in terms of the powers of the hyperfine interaction $\alpha_a(\omega) = \alpha_a^{(2)}(\omega) + \alpha_a^{(3)}(\omega) + \dots$. The leading term, $\alpha_a^{(2)}(\omega)$, contains the interaction with two photons and $\alpha_a^{(3)}(\omega)$ in addition involves the hyperfine coupling of the electrons with the nuclear spin. The relevant diagrams are shown in Fig. 1. It is important to realize that the scalar component of $\alpha_a^{(2)}(\omega)$ does not depend on F . Also for $J = 1/2$ levels, the tensor component of $\alpha_a^{(2)}(\omega)$ vanishes due to selection rules, as the underlying rotational symmetry is that of the rank 2 tensor. We conclude that for a $J = 1/2$ level in a laser light of linear polarization, the dominant Stark shift vanishes. Consequently, below we restrict consideration to the $J = 1/2$ levels.

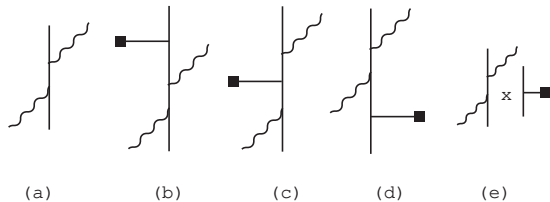


FIG. 1: Contributions to the dynamic polarizability $\alpha(\omega)$. Interactions with the laser photons are shown with wavy lines and hyperfine interaction with the capped solid line. (a) Second-order $\alpha^{(2)}(\omega)$. Contributions (b)–(e) are the third-order contributions to polarizabilities (b) top, (c) center, (d) bottom, and (e) normalization diagrams.

Since in the leading order both clock levels are shifted identically, we proceed to computing the third-order diagrams of Fig. 1. Each diagram involves two couplings to the lattice laser field and one hyperfine interaction (HFI). The labeling of the diagrams (top, center, and bottom) reflects the position of the HFI with respect to the two laser interactions. The formalism and the computational scheme is similar to those of Refs. [8, 9]. We carry out the conventional angular reduction and extract the scalar and tensor contributions to each diagram. We find that the third-order shift may be parameterized as

$$\delta\nu^{\text{Stark}}(\omega_L) = \left(\frac{1}{2}\mathcal{E}_0\right)^2 \left(A(F', F'') \left[\alpha_{n(IJ)F'}^{(3)}(\omega_L) \right]^{\text{Scalar}} + B(F', F'') \left[\alpha_{n(IJ)F'}^{(3)}(\omega_L) \right]^{\text{Tensor}} \right), \quad (2)$$

where coefficients $A(F', F'')$ and $B(F', F'')$ depend on the F -numbers of the clock states and on the orientation (\parallel or \perp) of the quantizing B-field with respect to the polarization vector of the laser light. The relation (2) arises due to the fact that the respective scalar and tensor parts of the dynamic polarizability vary proportionally for the two clock states. Clearly the scalar and tensor contributions to the differential shift must cancel each other at the magic wavelength.

We start with discussing the results for the metrologically important ^{133}Cs atom. A lattice Cs microwave

clock was discussed in Ref. [10]. Here the clock transition is between the $F = 4$ and $F = 3$ hyperfine components of the electronic ground state $6s_{1/2}$. Since $J = 1/2$, for linear polarization the second-order shift of the clock frequency vanishes and we need to proceed to the third-order diagrams, Fig. 1 (b)–(e). We carried out relativistic many-body calculations of these diagrams and found that there is no magic wavelength for the Cs clock. This is in contrast to findings of Ref. [10], where a multitude of magic wavelengths was identified. Qualitatively, for Cs, the tensor contribution to the clock shift is much smaller than the scalar contribution and this leads to unfavorable conditions for reaching the cancellation of the scalar and tensor shifts in Eq. (2).

We conclude that to cancel the third-order light shift we need to find atoms where the scalar and tensor shifts are comparable. This happens for atoms having the valence electrons in the $p_{1/2}$ state. For non-zero nuclear spin, the $p_{1/2}$ state has two hyperfine components that may serve as the clock states. Moreover, since the electronic angular momentum $J = 1/2$ for the linear polarization the leading second-order shift of the clock frequency vanishes. This is similar to the Cs $s_{1/2}$ case. The advantage of the $p_{1/2}$ state comes from the fact it is part of a fine-structure manifold: there is a nearby $p_{3/2}$ state separated by a relatively small energy interval determined by the relativistic corrections to the atomic structure. The hyperfine interaction between the states of the same manifold is amplified due to small energy denominators entering top and bottom diagrams of Fig. 1. The amplification occurs only for the tensor contribution. For the scalar contribution the intermediate state must be of the $p_{1/2}$ symmetry, whereas for the tensor contribution the intermediate state must be of the (strongly coupled) $p_{3/2}$ symmetry.

We illustrate this qualitative discussion with numerical examples for the group III atoms. We start with aluminum ($Z = 13$). The clock transition is between the hyperfine structure levels $F = 3$ and $F = 2$ in the ground $3p_{1/2}$ state of ^{27}Al isotope ($I = 5/2$). The clock frequency has been measured to be 1.50614(5) GHz [11], placing it in the microwave region. The μMagic clock setup requires ultracold atoms. Cooling Al has already been demonstrated [12] with the goal of atomic nanofabrication. The laser cooling was carried out on the closed $3p_{3/2} - 3d_{5/2}$ transition with the recoil limit of 7.5 μK . Once trapped, the atoms can be readily transferred from the metastable $3p_{3/2}$ cooling state to the ground (clock) state. Lattice-trapped Al was also considered for quantum information processing [13].

Using relativistic many-body theory we computed the polarizabilities for the two experimental geometries ($\mathbf{B} \parallel \hat{k}$ or $\mathbf{B} \parallel \hat{\varepsilon}$) and found three magic frequencies. For the $\mathbf{B} \parallel \hat{k}$ configuration the magic wavelengths and the second-order polarizabilities are

$$\begin{aligned} \lambda_L^* &= 390 \text{ nm}, \quad \alpha^S(\omega_L^*) = -211 \text{ a.u.}, \\ \lambda_L^* &= 338 \text{ nm}, \quad \alpha^S(\omega_L^*) = +142 \text{ a.u.}, \end{aligned}$$

and for the $\mathbf{B} \parallel \hat{\varepsilon}$ geometry

$$\lambda_L^* = 400 \text{ nm}, \alpha^S(\omega_L^*) = +401 \text{ a.u.}$$

The $3p_{1/2} - 4s_{1/2}$ transition is 394.5 nm, indicating a blue-detuning for the first two ($\mathbf{B} \parallel \hat{k}$) magic wavelengths and a red-detuning for the last one ($\mathbf{B} \parallel \hat{\varepsilon}$).

The third-order Stark shifts of the clock levels as a function of ω_L are shown in Fig. 2. At the magic wavelength the Stark shifts are identical and the clock transition is unperturbed. The cancellations between scalar and tensor contributions in Eq. (2) to the clock shift is illustrated in Fig. 3.

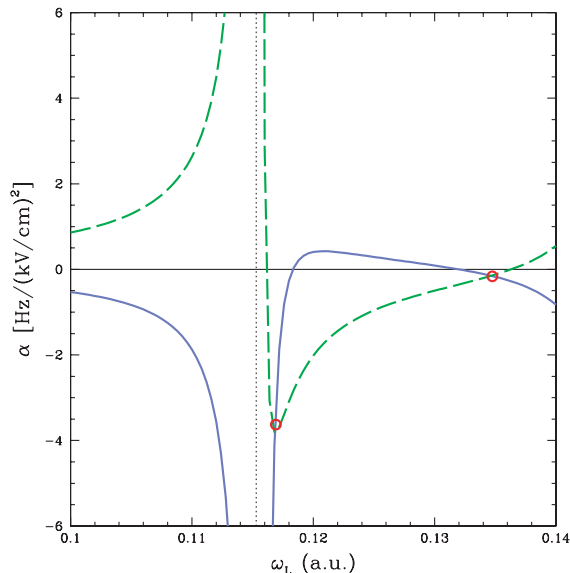


FIG. 2: (Color online) Third-order shift of the clock levels $|F = 3, M_F = 0\rangle$ (dashed line) and $|F = 2, M_F = 0\rangle$ (solid line) for Al μ Magic clock in the $\mathbf{B} \parallel \hat{k}$ geometry as a function of the lattice laser frequency. The shifts are identical at the magic frequencies (red circles) above the $3p_{1/2} - 4s_{1/2}$ resonance (vertical dotted line).

The values of polarizability $\alpha^S(\omega_L^*)$ determine the depths of the optical potentials. In general, a laser of intensity 10 kW/cm^2 would be able to hold atoms of temperature $10 \mu\text{K}$. The atoms are trapped in the intensity minima of the standing wave for $\alpha^S(\omega_L^*) < 0$ and in the maxima otherwise. Both cases are realized depending on the geometry. For the blue-detuned case, one could use hollow beams to confine atoms in the radial direction. We also notice that a 3D lattice can be formed by three sets of counter-propagating laser beams. In this case one pair operates in the $\mathbf{B} \parallel \hat{k}$ geometry and with the appropriate magic wavelength, while the orthogonal beams operate at the $\mathbf{B} \parallel \hat{\varepsilon}$ magic wavelength.

Presently, the factor limiting the accuracy of the most precise neutral-atom clocks is the black-body radiation (BBR), which arises due to an interaction of a thermal bath of photons at ambient temperature T with the

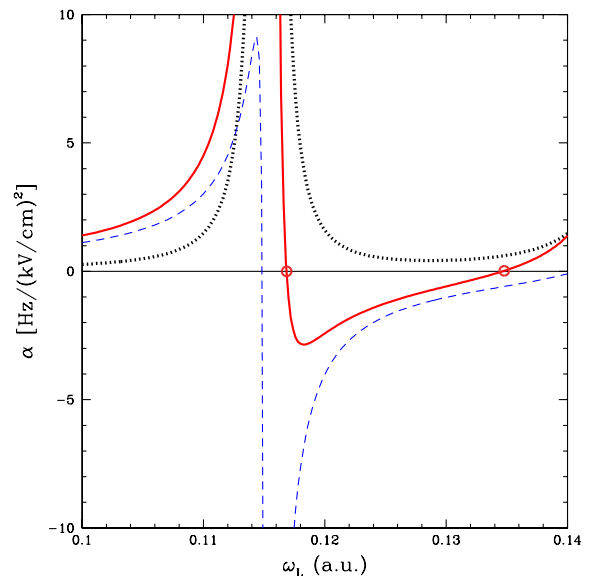


FIG. 3: (Color online) Differential polarizability for Al μ Magic clock in the $\mathbf{B} \parallel \hat{k}$ geometry as a function of the lattice laser frequency. Dotted line: contribution from scalar term; dashed line: contribution from the tensor term; solid line: total polarizability. Total clock shift vanishes at two values of the laser frequency.

clock [7, 14]. Due to the isotropic and low-frequency character of the BBR, the relevant shift involves only the scalar part of the polarizability evaluated in the static limit and given by the third-order diagrams of Fig. 1 (see formalism of Refs. [8, 9]). The fractional contribution is conventionally parameterized as

$$\frac{\delta\nu^{BBR}}{\nu_0} = \beta \left(\frac{T}{300} \right)^4,$$

where T is expressed in Kelvins. We find that our computed coefficient $\beta(^{27}\text{Al}) = -8.7 \times 10^{-16}$ is about 20 times smaller than the coefficient for the Cs standard. In other words, the Al μ Magic clock by an order of magnitude is less susceptible to the BBR than the primary standard. As β may be determined from experiments with static E-fields, we notice that ultimate accuracy of the clock is limited by an inhomogeneity of the BBR temperature across the experimental chamber. A typical inhomogeneity of 0.1 K results in an estimate of the fractional accuracy at 10^{-18} . As the BBR shift depends steeply on T , the entire experimental chamber could be cooled down cryogenically reducing the uncertainty even further; here the small volume of the chamber offers a distinct advantage over the fountain clocks [7].

While the choice of the $M_F = 0$ substates eliminates the first-order Zeeman shift, the sensitivity to B-fields comes through the second-order Zeeman shift which appears due to mixing of different hyperfine components by B : The relative shift of the clock frequency is

$\delta\nu^{\text{Zeeman}}/\nu_0 \approx 2/9 (\mu_B B/h\nu_0)^2 = 1.9 \times 10^{-7} B^2$, where B is expressed in Gauss. This problem is similar to that in the fountain clocks (Cs, Rb,...), where specific efforts to map the magnetic field over the flight zone are made. However, since in the lattice the atoms are confined to a tiny volume, one could control/shield the B-fields to a better degree than in the fountain clocks.

So far we assumed that the light is linearly polarized. In practice there is always a small degree of circular polarization \mathcal{A} present experimentally. The residual circular component leads to an undesired clock shift through axial (vector) dynamic polarizability α^v . This effect is equivalent to a “pseudo-magnetic” field along \hat{k} . For the $p_{1/2}$ clock levels α^v arises already in the second order; we find it to be in the order of 100 a.u. For the $M_F=0$ levels the relevant clock shift is zero in the first order in α^v . However, the shift could appear in the second order in $\mathcal{A}\alpha^v$ since the vector term mixes different hyperfine components. For a typical circular polarization $\mathcal{A} \sim 10^{-5}$ and a misalignment angle of 10^{-2} , the fractional frequency shift is just 10^{-21} .

Atoms of Al are bosons and the collisional clock shifts may become of issue, as in the fountain clocks [15, 16]. The advantage of the lattice clocks over the fountain clocks is that one could fill the lattice with no more than one atom per site, strongly suppressing the interatomic interactions and the associated shifts.

The scattering of the lattice laser photons leads to heating and reduces the interrogation time. At 10 kW/cm² the heating rate is in the order of 10^{-2} sec⁻¹. The heating can be suppressed by using the blue-detuned magic wavelength ($\lambda_L^* = 390$ nm), when the atoms are trapped at the intensity minima. This also reduces the effects of hyperpolarizability on the clock shift and multiphoton ionization rates.

We have carried out a similar analysis for Ga atom (both ⁶⁹Ga and ⁷¹Ga isotopes; $I = 3/2$), a member of the same group III of the periodic table as Al. Cooling

of this atom is pursued in atomic nanofabrication [17, 18]. The clock transition is between the hyperfine structure components $F = 1$ and $F = 2$ of the $4p_{1/2}$ ground state, and has been measured to be 2.6779875(10) GHz and 3.4026946(13) GHz for ⁶⁹Ga and ⁷¹Ga, respectively [19]. In contrast to Al, for this atom and the $M_F = 0$ sublevels, we have identified only a single magic wavelength at 450 nm in the $\mathbf{B} \parallel \hat{\varepsilon}$ geometry. This is red-detuned from the $4p_{1/2} - 5s_{1/2}$ transition frequency of 403.4 nm. We find $\alpha^S(\omega_L^*) = 94$ a.u. and a very small BBR coefficient $\beta(^{69,71}\text{Ga}) = -6.63 \times 10^{-17}$. We did not find the magic wavelengths for other group III atoms.

To summarize, we proposed Al and Ga microwave lattice clocks (μ Magic clocks). We calculated magic wavelengths for these clocks where the laser-induced differential Stark shift vanishes. This is a result of the opposite sign contributions of the scalar and tensor polarizabilities to the Stark shift. The tensor polarizability in the $p_{1/2}$ electron state is enhanced due to the mixing of $p_{1/2}$ and $p_{3/2}$ states by the hyperfine interaction. A similar mechanism for the magic wavelengths may work in microwave hyperfine transitions in other atoms which have the fine structure multiplets in the ground state. In atoms with the valence electron in the $s_{1/2}$ state (Cs, Rb, ...) the magic wavelength is absent. Estimates of the uncertainties show that the μ Magic clocks may successfully compete with the state of the art fountain clocks.

We gratefully acknowledge motivating discussion with P. Rosenbusch and invaluable advice of E.N. Fortson, S.A. Lee, H. Katori, J. Weinstein, J. Ye, P. Hannaford, N. Yu, and C. Salomon. AD was supported in part by the US Dept. of State Fulbright fellowship to Australia. This work was supported in part by the US National Science Foundation, by the Australian Research Council and by the US National Aeronautics and Space Administration under Grant/Cooperative Agreement No. NNX07AT65A issued by the Nevada NASA EPSCoR program.

-
- [1] S. Bize, P. Laurent, and M. Abgrall *et al.*, J. Phys. B **38**, S449 (2005).
[2] T. Heavner, S. Jefferts, E. Donley, and *et al.*, Metrologia **42**, 411 (2005).
[3] H. Katori, M. Takamoto, V. G. Pal’chikov, and V. D. Ovsiannikov, Phys. Rev. Lett. **91**, 173005 (2003).
[4] J. Ye, H. J. Kimble, and H. Katori, Science **320**, 1734 (2008).
[5] M. Takamoto, F. L. Hong, R. Higashi, and H. Katori, Nature (London) **435**, 321 (2005).
[6] R. Le Targat, X. Baillard, M. Fouché, A. Bruschi, O. Tcherbakoff, G. D. Rovera, and P. Lemonde, Phys. Rev. Lett. **97**, 130801 (2006).
[7] A. D. Ludlow, T. Zelevinsky, and G. K. Campbell *et al.*, Science **319**, 1805 (2008).
[8] K. Bely, U. I. Safronova, and A. Derevianko, Phys. Rev. Lett. **97**, 040801 (2006).
[9] E. J. Angstmann, V. A. Dzuba, and V. V. Flambaum, Phys. Rev. Lett. **97**, 040802 (2006).
[10] X. Zhou, X. Chen, and J. Chen (2005), arXiv:0512244.
[11] H. Lew and G. Wessel, Phys. Rev. **90**, 1 (1953).
[12] R. W. McGowan, D. M. Giltner, and S. A. Lee, Opt. Lett. **20**, 2535 (1995).
[13] B. Ravaine, A. Derevianko, and P. R. Berman, Phys. Rev. A **74**, 022330 (2006).
[14] S. G. Porsev and A. Derevianko, Phys. Rev. A **74**, 020502(R) (2006).
[15] F. Pereira Dos Santos, H. Marion, S. Bize, Y. Sortais, A. Clairon, and C. Salomon, Phys. Rev. Lett. **89**, 233004 (2002).
[16] K. Szymaniec, W. Chalupczak, E. Tiesinga, C. J. Williams, S. Weyers, and R. Wynands, Phys. Rev. Lett. **98**, 153002 (2007).
[17] S. J. Rehse, K. M. Bockel, and S. A. Lee, Phys. Rev. A **69**, 063404 (2004).
[18] A. Camposo, O. Marago, B. Fazio, B. Kloter,

D. Meschede, U. Rasbach, C. Weber, and E. Arimondo, Appl. Phys. B **85**, 487 (2006).

[19] A. Lurio and A. G. Prodel, Phys. Rev. **101**, 79 (1956).